DEVELOPMENT OF $Na_{0.7}Ni_{0.6}Mn_{0.2}Co_{0.2}O_2$ EMPLOYING SOL-GEL APPROACH AS CATHODE MATERIAL FOR SODIUM ION BATTERIES

Tien Phat Doan[1], Van Nguyen To[1], Van Tuan Nguyen[1], Viet Linh Pham[1], Trung Son Luong[1], Van Nghia Nguyen[2], Thi Lan Ngo[1,*]

[1]*Faculty of Physics and Chemical Engineering, Le Quy Don Technical University, Hanoi, Vietnam*

[2]*Hanoi Architectural University*

Abstract

Layered structural materials based on alkali metal oxide - transition metal oxide compositions are under scrutiny as promising candidates for positive electrodes in sodium ion batteries. In this study, we have successfully synthesized $Na_{0.7}Ni_{0.6}Mn_{0.2}Co_{0.2}O_2$ utilizing the sol-gel method in conjunction with calcination processes. The findings reveal that the synthesized material exhibits a P3 structure ideally suited for deployment as a positive electrode in sodium ion batteries. The material $Na_{0.7}Ni_{0.6}Mn_{0.2}Co_{0.2}O_2$ demonstrates a peak specific capacity of 109.0 mAh g^{-1} at a current density of 5 mA g^{-1}, retaining 66.8% of this capacity following 50 consecutive charge-discharge cycles at a current density of 10 mA g^{-1}. These outcomes indicate the potential of the developed $Na_{0.7}Ni_{0.6}Mn_{0.2}Co_{0.2}O_2$ material as a viable candidate for cathode fabrication in sodium ion batteries, showcasing promising performance characteristics for future battery applications.

Keywords: *Sodium ion battery; alkali metal oxide - transition metal oxide; sol-gel method.*

1. Introduction

Sodium ion rechargeable batteries have emerged as a promising alternative to lithium ion batteries for large-scale energy storage systems, owing to the abundant supply of sodium and its similar physicochemical properties to lithium [1]. However, challenges such as the larger atomic radius and higher density of sodium present barriers affecting the specific capacity, cycle life, and charge-discharge rates of sodium ion batteries compared to lithium counterparts. It is therefore, enhancing electrode materials, particularly positive electrode materials, is crucial for optimizing battery performance.

Among positive electrode materials, alkali metal oxide materials combined with transition metals in an AMO_2 layer structure (where, A represents alkali metals such as Li, Na, K; M represents transition metals such as Mn, Co, Ni, Fe,...) have garnered attention for their potential to offer superior specific capacity and durability compared to

* Email: ngothilan@lqdtu.edu.vn

DOI: 10.56651/lqdtu.jst.v2.n01.768.pce

other materials [1, 2]. These materials AMO_2 are categorized into O3 and P2 structural groups, with sodium ions positioned between transition metal oxide layers in octahedral and prismatic arrangements, respectively [3-6] and most of them are often prepared at temperatures greater than 850ºC [7]. In recent years, P3 structured materials have emerged as a more efficient, energy-saving alternative to P2 and O3 structured materials due to their lower synthesis temperatures [7, 8].

Literature suggest that manganese is commonly favored for positive electrode materials in sodium ion batteries, yet its extensive use poses challenges for post-use recovery in commercial products [3, 9]. Therefore, minimizing manganese utilization while increasing the presence of easily recoverable transition metals without compromising electrochemical performance holds significant scientific importance. Nickel, being abundant in the Earth's crust and readily recoverable, has garnered interest for enhancing positive electrode materials in sodium ion batteries. Noteworthy studies focusing on enhancing the utilization of nickel as a positive electrode material in sodium ion rechargeable batteries include: (i) $NaNiO_2$ exhibiting a capacity of 130 mAh g^{-1} and retaining 84% capacity after 5 charge-discharge cycles [10]. $Na_{0.85}Li_{0.12}Ni_{0.22}Mn_{0.88}O_2$ demonstrating a specific capacity of up to 124 mAh g^{-1} and maintaining 85.4% capacity after 500 cycles at high current density (5C) [11]; P2/P3-$Na_{0,7}Co_{0,5}Mn_{0,33}Ni_{0,36}O_2$ exhibiting a capacity of 120 mAh g^{-1} and retaining 67% capacity after 100 charge-discharge cycles [12].

This study focuses on synthesizing $Na_{0.7}Ni_{0.6}Mn_{0.2}Co_{0.2}O_2$ through the sol-gel method coupled with calcination process. Material characterization involves advanced physicochemical techniques such as X-ray diffraction (XRD), scanning electron microscopy (SEM), energy-dispersive X-ray spectroscopy (EDS), galvanostatic charge-discharge (GCD) analysis and cyclic voltammetry (CV).

2. Experimental details

2.1. Chemicals

The chemicals employed in the study comprise sodium acetate CH_3COONa (Xilong, China), Nickel(II) acetate tetrahydrate $Ni(CH_3COO)_2.4H_2O$ (Xilong, China), Manganese(II) acetate tetrahydrate $Mn(CH_3COO)_2.4H_2O$ (Xilong, China), Cobalt(II) acetate tetrahydrate $Co(CH_3COO)_2.4H_2O$ (Xilong, China), Citric acid monohydrate $C_6H_8O_7.H_2O$ (Xilong, China), Lithium perchlorate $LiClO_4$ (Alfa Aesar), Superconducting Carbon (Supper P) (Alfa Aesar), Poly vinylidene fluoride (PVDF) (Alfa Aesar), N-methyl-2-pyrrolidone (NMP) (Alfa Aesar), Ethylene carbonate (EC) (Sigma - Aldrich), and Diethyl carbonate (Sigma - Aldrich). These chemicals were of analytical grade and used without further purification.

2.2. Material fabrication

The initial step in fabricating sample is to prepare the raw material by weighing out 2.378 g of CH_3COONa (29 mmol), 5.973 g of $Ni(CH_3COO)_2.4H_2O$ (24 mmol), 1.961 g of $Mn(CH_3COO)_2.4H_2O$ (8 mmol), 1.993 g of $Co(CH_3COO)_2.4H_2O$ (8 mmol), and 21.014 g of $C_6H_8O_7.H_2O$ (100 mmol). In addition, a slightly exceed of the required amount of CH_3COONa salt by 4% was taken into account to compensate potential sodium ion loss during thermal decomposition.

The next step is to initiate the intricate process by combining the precursor mixture in a pristine glass vessel. Then a gradual introduction of distilled water until attaining a volume of 100 mL is performed and ensured continuous stir at an elevated temperature of 80°C, which facilitates the formation of a homogeneous gel. To obtain the desired xerogel, the gel is subjected to a dehydration process within a precisely regulated oven maintained at 120°C. Subsequently, the xerogel is further exposed to a thermal treatment at 400°C for a duration of 2 hours, fostering structural transformations. The heat-treated material is now transferred to a high-temperature ceramic crucible, where it undergoes further heating at an elevated temperature of 600°C for an additional 2 hours.

Uniform pellets are formed by compacting the thermally processed material, which are ready for the final calcination stage. These pellets are subjected to an intense heat treatment at 850°C, maintained for an extended period of 20 hours. This rigorous calcination process ensures the complete removal of residual impurities and the stabilization of the material. The intricate details of this meticulously designed fabrication protocol are vividly depicted in Fig. 1, serving as a comprehensive visual reference.

2.3. Material characterization approaches

• *Characteristics:*

The crystal structure analysis was conducted using X-ray diffraction (XRD) on a Bruker D8 X-ray diffractometer, utilizing the K-α1 wavelength of a copper electrode. The morphology and composition analysis were performed using scanning electron microscopy (SEM) coupled with X-ray energy dispersive spectroscopy (EDS) on a Hitachi S-4800.

• *Electrochemical Properties:*

Following fabrication, the materials were utilized to fabricate the working electrode. A uniform mortar was prepared by blending the active material, superconducting carbon (Supper P), and PVDF in a mass ratio of 80:10:10, dissolved in N-methyl-2-pyrrolidone (NMP) solvent. This mixture was evenly spread onto a 15 μm thick aluminum foil and dried at 100°C in a vacuum oven for 12 hours. Subsequently, the electrode was cut into sheets conforming to CR2032 battery standards.

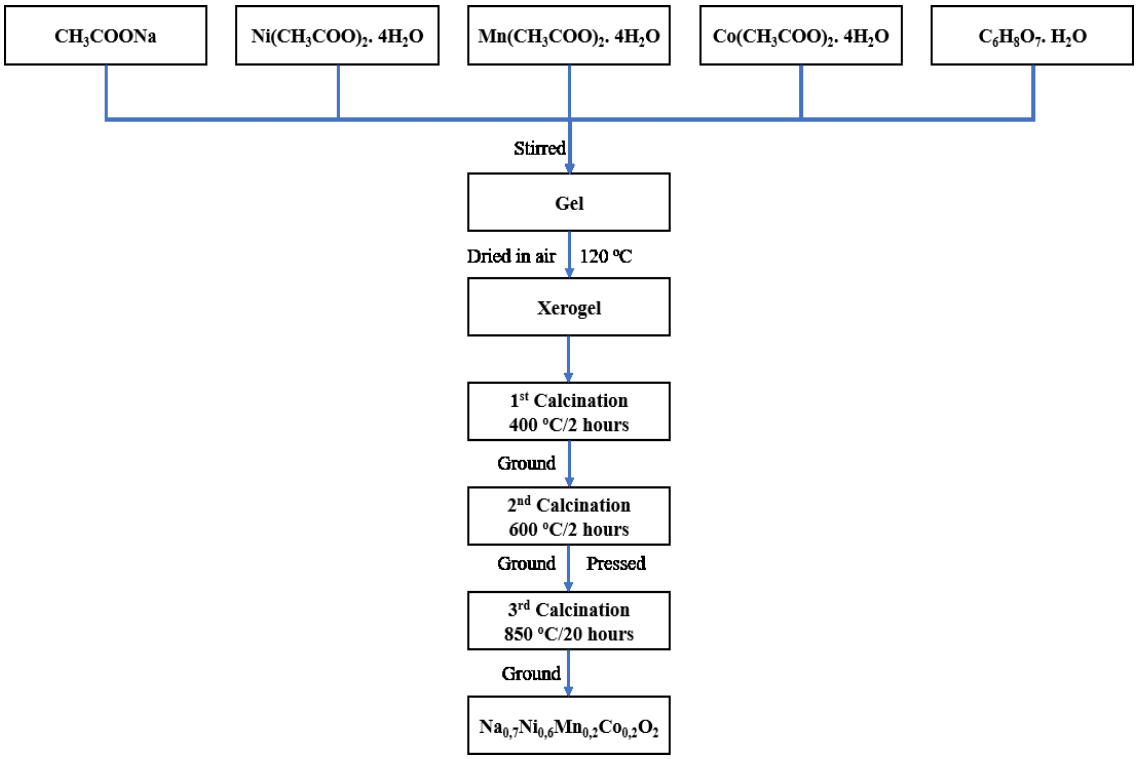

Fig. 1. Procedure in fabricating $Na_{0.7}Ni_{0.6}Mn_{0.2}Co_{0.2}O_2$ material.

2.4. Material characterization approaches

• *Characteristics:*

The crystal structure analysis was conducted using X-ray diffraction (XRD) on a Bruker D8 X-ray diffractometer, utilizing the K-α1 wavelength of a copper electrode. The morphology and composition analysis were performed using scanning electron microscopy (SEM) coupled with X-ray energy dispersive spectroscopy (EDS) on a Hitachi S-4800.

• *Electrochemical properties:*

Following fabrication, the materials were utilized to fabricate the working electrode. A uniform mortar was prepared by blending the active material, superconducting carbon (Supper P), and PVDF in a mass ratio of 80:10:10, dissolved in N-methyl-2-pyrrolidone (NMP) solvent. This mixture was evenly spread onto a 15 µm thick aluminum foil and dried at 100°C in a vacuum oven for 12 hours. Subsequently, the electrode was cut into sheets conforming to CR2032 battery standards.

The CR2032 sodium-ion battery assembly was carried out within an argon-filled glove box with O_2 and H_2O concentrations maintained below 0.1 ppm. The battery configuration included a working electrode composed of $Na_{0.7}Ni_{0.6}Mn_{0.2}Co_{0.2}O_2$, a metallic Sodium foil counter electrode, a polypropylene (PP) film separator, and a 1M $NaClO_4$ electrolyte solution in an ethylene carbonate/diethyl carbonate mixture (EC/DEC, 1:1 by volume).

The electrochemical performance assessment of the $Na_{0.7}Ni_{0.6}Mn_{0.2}Co_{0.2}O_2$ material was conducted using a conventional button-type Na-ion battery employing the constant current charge and discharge (GCD) method on a NEWARE automatic discharge device.

3. Results and discussion

The crystallographic arrangement of the compound $Na_{0.7}Ni_{0.6}Mn_{0.2}Co_{0.2}O_2$, hereinafter referred to as NaNMC, is visually depicted in Fig. 2. The distinctive diffraction patterns of this material manifest at specific angles of 2θ: 16.0; 32.3; 36.8; 38.0; 42.6; 45.8; 53.6; 58.0; 65.6 and 68.0^o, corresponding to the crystal lattice planes (003), (006), (101), (012), (104), (015), (107), (018), (110) and (1010).

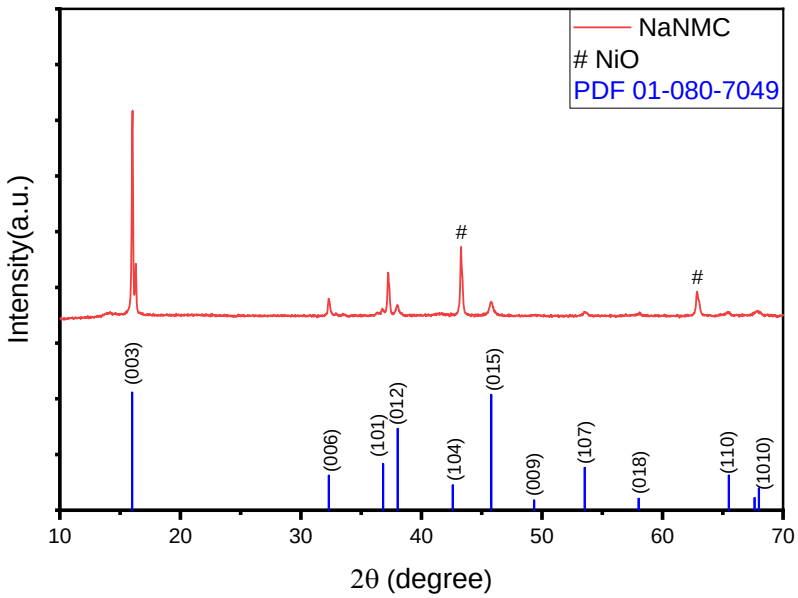

Fig. 2. XRD patterns of the NaNMC material in θ - 2θ configuration.

The X-ray diffraction pattern of NaNMC aligns perfectly with the reference card No PDF 01-080-7049, illustrating a prismatic - trigonal P3 structure within the space group $R3m$. These diffraction peaks agree well with those observed in similar P3 materials from previous studies [7, 12-14]. The sharp and distinct diffraction peaks in the XRD pattern affirm the exceptional crystallinity of the synthesized material. Notably, a minor NiO impurity peak at 2θ = 43.3; 62.9° is detected, attributed to the high instability of Ni^{3+} compared to Co^{3+} and Mn^{3+} and this was also discussed in previous studies [12, 15].

The morphology analysis via scanning electron microscopy (SEM) reveals a well-defined layered structure of NaNMC, with particle sizes varying widely and exhibiting tendencies to agglomerate, as evidenced in Fig. 3a and Fig. 3b. High magnification SEM

image (Fig. 3b) unveils secondary particles comprising smaller primary particles ranging from 100 nm to 200 nm, closely compacted together due to surface melting at 850°C of the primary particles.

The elemental composition of NaNMC is confirmed through X-ray energy dispersive spectroscopy (EDS), as depicted in Fig. 3c, revealing the presence of all interested Na, Ni, Mn, Co, and O elements in the NaNMC material. The Ni/Mn/Co ratio of 15.34/5.20/5.19, corresponding to 5.91/2/2 in NaNMC closely matches the initial salt mixture ratio of $Ni^{2+}/Mn^{2+}/Co^{2+}$ elments, while slight deviations, i.e., 8.17/6 vs the initial value of 7/6, in the Na/Ni ratio are attributed to the EDS measurement errors.

The comprehensive analyses from XRD, SEM, and EDS approve the successful synthesis of $Na_{0.7}Ni_{0.6}Mn_{0.2}Co_{0.2}O_2$ with high purity, although the presence of NiO impurity might influence its electrochemical performance.

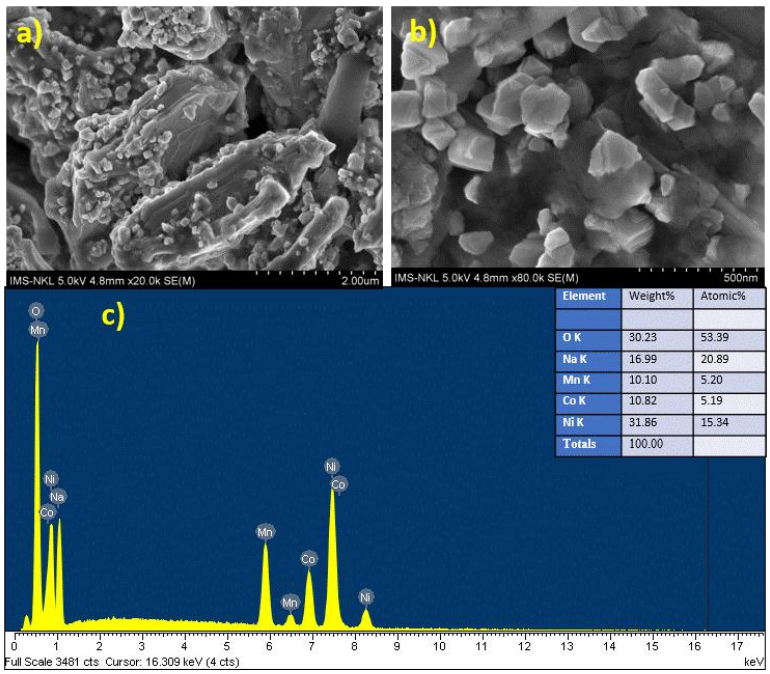

Fig. 3. The SEM morphologies of the developed NaNMC material with low (a) and high (b) magnification, accompanied by the EDS spectra.

In this investigation, the electrochemical performance of the newly developed material was assessed using the constant current charge-discharge (GCD) technique. The charge-discharge profiles for the initial three cycles, conducted at a current density of 5 mA g^{-1}, are depicted in Fig. 4a. The specific capacities for these initial cycles are about 105.6, 109.0, and 108.6 mAh g^{-1}, respectively. However, these values fall below the

specific capacity of 146 mAh/g achieved by the same material synthesized via the co-precipitation method at a current density of 0.1 C [16]. The material synthesized in that study exhibits a P2 crystal structure, known for its enhanced stability compared to the P3 structure referenced in previous results [12]. In comparison to other P3-type materials like P3-$Na_{0.67}Mn_{0.67}Ni_{0.33}O_2$ with capacities of 100 mAh g^{-1} in the potential range 4.1 - 2.0 V and 230 mAh g^{-1} in the potential range 4.5 - 1.5 V [7]; P3-$Na_{0.75}Mn_{0.75}Ni_{0.25}O_2$ with a capacity of 190 mAh g^{-1} in the potential range 4.5 - 1.5 V [13]. This discrepancy in capacity could be attributed to the presence of NiO impurities in the synthesized material, indicating a lack of complete single-phase formation and impacting its overall performance.

Figure 4b illustrates the GCD curves at various current densities (5 mA g^{-1}, 10 mA g^{-1}, 20 mA g^{-1}, 50 mA g^{-1}, and 100 mA g^{-1}), at which the charge-discharge rate of the developed materials are evaluated. The findings reveal a notable decline in discharge specific capacity with escalating current density. Specifically, the discharge specific capacity of NaNMC material diminishes significantly with increasing current density, registering values of 109.0, 103.5, 91.6, 55.7, and 14.8 mAh g^{-1} at 5 mA g^{-1}, 10 mA g^{-1}, 20 mA g^{-1}, 50 mA g^{-1}, and 100 mA g^{-1}, respectively. The reduction in specific capacity as current density rises is intricately linked to the electrochemical reaction kinetics within the battery, i.e., optimal efficiency is achieved during slower reactions [17]. This observation underscores that the NaNMC material synthesized in this study is best suited for charging and discharging operations at lower current densities.

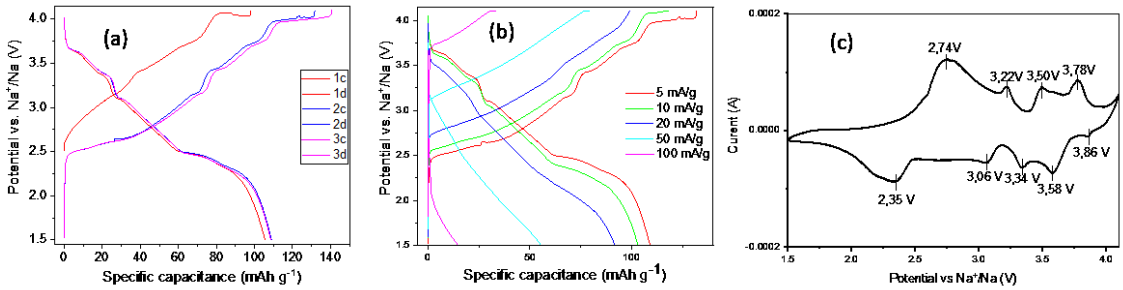

Fig. 4. The GCD of charge-discharge curves of developed NaNMC material: (a) three initial cycles at a current density of 5 mA g-1, (b) at various current density, and (c) the cyclic voltammogram of NaNMC.

Figure 4c illustrates the cyclic voltammogram of NaNMC at a scan rate of 0.05 mV s^{-1} in the voltage range from 1.5 to 4.1 V. The CV curves of NaNMC sample appear four anodic peaks (at about 2.74 V, 3.22 V, 3.50 and 3.78 V) for charge process and five cathodic peaks (at about 2.35 V, 3.06 V, 3.34V, 3.58 V and 3.86 V) for discharge process.

These characteristics are consistent with the characteristics of the above GCD charge-discharge path, typical of materials with P3 structure found in the previous report [11].

In order to assess the cyclic behavior of the NaNMC material, a series of 50 consecutive charge-discharge cycles were conducted at varying current densities and at a certain current density, as depicted in Fig. 5. Figure 5a reveals not only a notable decline in the specific capacity of the NaNMC material as the current density escalates from low level to the higher one, but also a significant drop observed at specific current levels. Following 35 cycles across diverse current densities, the remaining NaNMC material exhibited a specific capacity of 100.5 mAh/g, equivalent to 95.2% of the initial cycle's capacity.

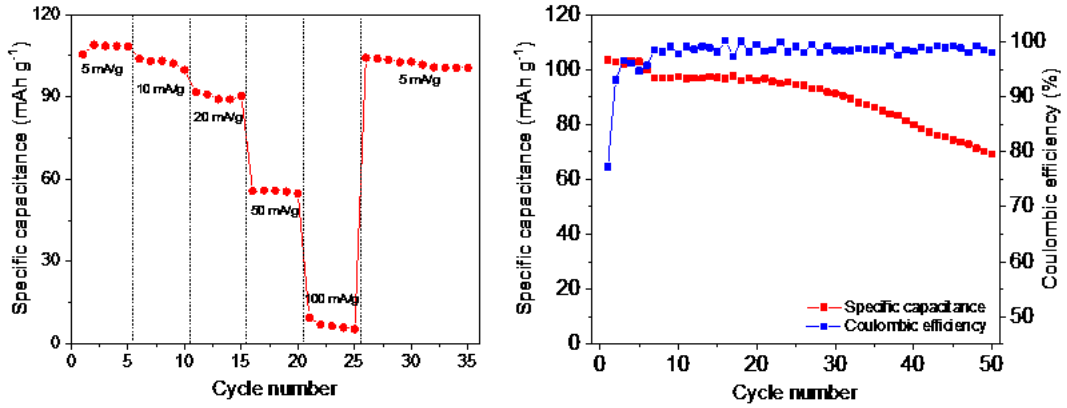

a) *b)*

Fig. 5. Cyclic performance of the developed NaNMC material: (a) at various current densities, and (b) at a certain current density of 10 mA g^{-1}.

Figure 5b illustrates the electrochemical performance evaluation of the material after 50 cycles at a constant current density of 10 mAh g^{-1}. The findings indicate a rapid decrease in discharge specific capacity to 69.1 mAh g^{-1} (66.8% of the initial cycle's capacity) after 50 charge-discharge cycles, while the coulombic efficiency remained stable at approximately 98%. This swift capacity reduction is attributed to the characteristics of the P3 structural material.

The dynamic phase transitions of the P3 structural material during charge and discharge operations introduce a substantial energy barrier, impeding the movement of Na+ ions, as elucidated in previous studies [7, 13]. These electrochemical traits suggest

the imperative need for enhancing both structural stability and reversibility during the sodium ion exchange process of NaNMC material.

4. Conclusion

Layered structural materials derived from transition metal oxide $Na_{0.7}Ni_{0.6}Mn_{0.2}Co_{0.2}O_2$ have been effectively fabricated through the sol-gel method accompanied by calcination process. The synthesised material exhibits a specific discharge capacity of 109.0 mAh at a current density of 5 mA g^{-1}. Following 50 consecutive charge and discharge cycles at a current density of 10 mA g^{-1}, the discharge specific capacity of the material is maintained at 66.8% compared to the initial cycle value. These results, while promising, reveal limitations compared to analogous materials, highlighting the necessity for further enhancements in structural stability to elevate the electrochemical performance of the material.

Acknowledgments

This research is funded by Vietnam National Foundation for Science and Technology Development (NAFOSTED) under grant number NCUD.01-2022.03.

References

[1] J. Choi, K. H. Kim, C. H. Jung, and S. H. Hong, "A P2-type $Na_{0.7}(Ni_{0.6}Co_{0.2}Mn_{0.2})O_2$ cathode with excellent cyclability and rate capability for sodium ion batteries", *Chemical Communications*, Vol. 55 (77), pp. 11575-11578, 2019.

[2] R. Fielden and M. N. Obrovac, "Investigation of the $NaNi_xMn_{1-x}O_2$ ($0 \leq x \leq 1$) system for Na-ion battery cathode materials", *Journal of the Electrochemical Society*, 162 (3), A453, 2015.

[3] H. Guo, M. Avdeev, K. Sun, …, D. Chen, "Pentanary transition-metals Na-ion layered oxide cathode with highly reversible O3-P3 phase transition", *Chemical Engineering Journal*, 412, 2021, 128704. DOI: 10.1016/j.cej.2021.128704

[4] C. Hakim, H. D. Asfaw, R. Younesi, …, I. Saadoune, "Development of P2 or P2/P3 cathode materials for sodium-ion batteries by controlling the Ni and Mn contents in $Na_{0.7}Co_xMn_yNi_zO_2$ layered oxide", *Electrochimica Acta*, Vol. 438, 2023, 141540.

[5] I. Hasa, S. Mariyappan, D. Saurel, …, M. Casas-Cabanas "Challenges of today for Na-based batteries of the future: From materials to cell metrics", *Journal of Power Sources*, Vol. 482, 2021, 228872.

[6] J. Y. Hwang, S. T. Myung, and Y. K. Sun, "Sodium-ion batteries: present and future", *Chemical Society Reviews*, Vol. 46 (12), pp. 3529-3614, 2017.

[7] T. Jin, P. F. Wang, Q. C. Wang, …, C. Wang "Realizing Complete Solid-Solution Reaction in High Sodium Content P2-Type Cathode for High-Performance Sodium-Ion Batteries", *Angewandte Chemie - International Edition*, Vol. 59 (34), pp. 14511-14516, 2020. DOI: 10.1002/anie.202003972

[8] R. Luo, F. Wu, M. Xie, …, R. Chen, "Habit plane-driven P2-type manganese-based layered oxide as long cycling cathode for Na-ion batteries", *Journal of Power Sources*, Vol. 383, pp. 80-86, 2018.

[9] X. Ma, C. Yang, Z. Xu, …, Y. Jin, "Structural and electrochemical progress of O3-type layered oxide cathodes for Na-ion batteries", *Nanoscale*, Vol. 15 (36), pp. 14737-14753, 2023.

[10] N. Q. Quyen, T. Van Nguyen, H. H. Thang, P. M. Thao, and N. Van Nghia, "Carbon coated $NaLi_{0.2}Mn_{0.8}O_2$ as a superb cathode material for sodium ion batteries", *Journal of Alloys and Compounds*, Vol. 866, 2021, 158950. DOI: 10.1016/j.jallcom.2021.158950

[11] H. N. Vasavan, M. Badole, S. Saxena, …, S. Kumar, "Unveiling the potential of P3 phase in enhancing the electrochemical performance of a layered oxide cathode", *Materials Today Energy*, Vol. 37, 2023, 101380.

[12] L. Wang, J. Wang, X. Zhang, …, J. Wang, "Unravelling the origin of irreversible capacity loss in $NaNiO_2$ for high voltage sodium ion batteries", *Nano Energy*, Vol. 34(January), pp. 215-223, 2017. DOI: 10.1016/j.nanoen.2017.02.046

[13] P. Wang, H. Yao, X. Liu, …, Y. Guo, "Ti-substituted $NaNi_{0.5}Mn_{0.5-x}Ti_xO_2$ cathodes with reversible O3-P3 phase transition for high-performance sodium-ion batteries", *Advanced Materials*, Vol. 29 (19), 2017, 1700210.

[14] L. Yang, X. Li, J. Liu, …, H. Chen, "Lithium-Doping Stabilized High-Performance P2-$Na_{0.66}Li_{0.18}Fe_{0.12}Mn_{0.7}O_2$ Cathode for Sodium Ion Batteries", *Journal of the American Chemical Society*, Vol. 141(16), pp. 6680-6689, 2019. DOI: 10.1021/jacs.9b01855

[15] L. Zhang, J. Wang, J. Li, …, G. Schumacher, J. Li, "Preferential occupation of Na in P3-type layered cathode material for sodium ion batteries", *Nano Energy*, Vol. 70, 2020, 104535.

[16] R. Zhang, Z. Lu, Y. Yang, and W. Shi, "First-principles investigation of the monoclinic $NaMnO_2$ cathode material for rechargeable Na-ion batteries", *Current Applied Physics*, Vol. 18 (11), pp. 1431-1435, 2018. DOI: 10.1016/j.cap.2018.08.011

[17] D. Zhou, W. Huang, and F. Zhao, "P2-type $Na_{0.67}Fe_{0.3}Mn_{0.3}Co_{0.4}O_2$ cathodes for high-performance sodium-ion batteries", *Solid State Ionics*, Vol. 322, pp. 18-23, 2018.

TỔNG HỢP $Na_{0,7}Ni_{0,6}Mn_{0,2}Co_{0,2}O_2$ BẰNG PHƯƠNG PHÁP SOL-GEL ỨNG DỤNG LÀM VẬT LIỆU ĐIỆN CỰC DƯƠNG CHO PIN ION NATRI

Đoàn Tiến Phát[1], Tô Văn Nguyện[1], Nguyễn Văn Tuấn[1], Phạm Việt Linh[1], Lương Trung Sơn[1], Nguyễn Văn Nghĩa[2], Ngô Thị Lan[1]

[1]*Khoa Hóa - Lý kỹ thuật, Trường Đại học Kỹ thuật Lê Quý Đôn, Hà Nội, Việt Nam*

[2]*Trường Đại học Kiến trúc Hà Nội*

Tóm tắt: Vật liệu cấu trúc lớp trên cơ sở oxit kim loại kiềm - oxit kim loại chuyển tiếp được đánh giá là loại vật liệu tiềm năng làm điện cực dương cho pin ion natri. Trong nghiên cứu này, chúng tôi đã tổng hợp thành công vật liệu $Na_{0,7}Ni_{0,6}Mn_{0,2}Co_{0,2}O_2$ bằng phương pháp sol-gel kết hợp với nung. Kết quả chỉ ra rằng, vật liệu tổng hợp được có cấu trúc P3 phù hợp làm điện cực dương cho pin ion natri. Vật liệu $Na_{0,7}Ni_{0,6}Mn_{0,2}Co_{0,2}O_2$ có dung lượng riêng cực đại đạt 109,0 mAh/g tại mật độ dòng 5 mA/g. Vật liệu cũng duy trì được 66,8% dung lượng sau 50 chu kỳ nạp xả liên tục tại mật độ dòng 10 mA/g. Với những kết quả này, vật liệu $Na_{0,7}Ni_{0,6}Mn_{0,2}Co_{0,2}O_2$ được tổng hợp bằng phương pháp sol-gel kết hợp với nung hứa hẹn là vật liệu tiềm năng để chế tạo điệc cực dương cho pin ion natri.

Từ khóa: *Pin ion natri; oxit kim loại kiềm - oxit kim loại chuyển tiếp; phương pháp sol-gel.*

Received: 06/04/2024; Revised: 17/05/2024; Accepted for publication: 20/05/2024

❑